Pflugers Arch - Eur J Physiol (2017) 469:91–103
DOI 10.1007/s00424-016-1913-7

INVITED REVIEW

Common variants in *CLDN14* are associated with differential excretion of magnesium over calcium in urine

Tanguy Corre[1,2,3] · Eric Olinger[4] · Sarah E. Harris[5,6] · Michela Traglia[7] · Sheila Ulivi[8] · Stefania Lenarduzzi[8] · Hendrica Belge[4] · Sonia Youhanna[4] · Natsuko Tokonami[4] · Olivier Bonny[9] · Pascal Houillier[10,11] · Ozren Polasek[12,13] · Ian J. Deary[5,14] · John M. Starr[5,15] · Daniela Toniolo[7] · Paolo Gasparini[16,17] · Peter Vollenweider[9] · Caroline Hayward[18] · Murielle Bochud[1] · Olivier Devuyst[4]

Received: 23 September 2016 / Accepted: 22 November 2016 / Published online: 3 December 2016

Abstract The nature and importance of genetic factors regulating the differential handling of Ca^{2+} and Mg^{2+} by the renal tubule in the general population are poorly defined. We conducted a genome-wide meta-analysis of urinary magnesium-to-calcium ratio to identify associated common genetic variants. We included 9320 adults of European descent from four genetic isolates and three urban cohorts. Urinary magnesium and calcium concentrations were measured centrally in spot urine, and each study conducted linear regression analysis of urinary magnesium-to-calcium ratio on ~2.5 million

Tanguy Corre and Eric Olinger jointly contributed

Caroline Hayward, Murielle Bochud, and Olivier Devuyst jointly directed the study

Electronic supplementary material The online version of this article (doi:10.1007/s00424-016-1913-7) contains supplementary material, which is available to authorized users.

✉ Olivier Devuyst
olivier.devuyst@uzh.ch

[1] Institute of Social and Preventive Medicine, Lausanne University Hospital, Lausanne, Switzerland

[2] Department of Computational Biology, University of Lausanne, Lausanne, Switzerland

[3] Swiss Institute of Bioinformatics, Lausanne, Switzerland

[4] Institute of Physiology, University of Zurich, Winterthurerstrasse 190, CH-8057 Zürich, Switzerland

[5] Centre for Cognitive Ageing and Cognitive Epidemiology, University of Edinburgh, Edinburgh, UK

[6] Medical Genetics Section, University of Edinburgh Centre for Genomic and Experimental Medicine and MRC Institute of Genetics and Molecular Medicine, Western General Hospital, Edinburgh, UK

[7] Division of Genetics and Cell Biology, San Raffaele Scientific Institute, Milan, Italy

[8] Institute for Maternal and Child Health-IRCCS "Burlo Garofolo", Trieste, Italy

[9] Department of Medicine, Lausanne University Hospital, Lausanne, Switzerland

[10] INSERM U1138, Centre de Recherche des Cordeliers, Paris, France

[11] Département de Physiologie, Assistance Publique-Hôpitaux de Paris, Hôpital Européen Georges Pompidou, Paris, France

[12] Faculty of Medicine, University of Split, Split, Croatia

[13] Centre for Population Health Sciences, University of Edinburgh, Edinburgh, UK

[14] Department of Psychology, University of Edinburgh, Edinburgh, UK

[15] Alzheimer Scotland Dementia Research Centre, University of Edinburgh, Edinburgh, UK

[16] Department of Medical, Surgical and Health Sciences, University of Trieste, Trieste, Italy

[17] Department of Experimental Genetics, Sidra Medical and Research Center, Doha, Qatar

[18] MRC IGMM, University of Edinburgh, Edinburgh, UK

single-nucleotide polymorphisms (SNPs) using an additive model. We investigated, in mouse, the renal expression profile of the top candidate gene and its variation upon changes in dietary magnesium. The genome-wide analysis evidenced a top locus (rs172639, $p = 1.7 \times 10^{-12}$), encompassing *CLDN14*, the gene coding for claudin-14, that was genome-wide significant when using urinary magnesium-to-calcium ratio, but not either one taken separately. In mouse, claudin-14 is expressed in the distal nephron segments specifically handling magnesium, and its expression is regulated by chronic changes in dietary magnesium content. A genome-wide approach identified common variants in the *CLDN14* gene exerting a robust influence on the differential excretion of Mg^{2+} over Ca^{2+} in urine. These data highlight the power of urinary electrolyte ratios to unravel genetic determinants of renal tubular function. Coupled with mouse experiments, these results support a major role for claudin-14, a gene associated with kidney stones, in the differential paracellular handling of divalent cations by the renal tubule.

Keywords Tubular functions · Mg/Ca ratio · Claudin-14 · GWAS

Introduction

The kidneys play a major role in the homeostasis of calcium and magnesium: In steady state, approximately 98% of the filtrated Ca^{2+} and 95–99% of the filtrated Mg^{2+} are reabsorbed by the nephron. The handling of Ca^{2+} and Mg^{2+} involves a transcellular pathway, mediated by specific transporters expressed in the apical and basolateral membrane domains, and a paracellular pathway depending on transepithelial electrochemical gradients and regulated by specialized junctional proteins, the claudins. The claudins belong to a family of membrane-spanning tight junction proteins, which interact with scaffolding proteins and with other claudins to form pores and barriers regulating the permeability and selectivity of the paracellular pathway [48].

A dozen claudins are differentially expressed along the renal tubule, reflecting specific paracellular properties of each segment. The proximal tubule reabsorbs the bulk of filtered Ca^{2+} through the paracellular pathway involving claudin-2 [3, 30, 48]. In contrast, only 10–20% of the filtered Mg^{2+} is reabsorbed by that segment [6]. The thick ascending limb (TAL) of the loop of Henle mediates the paracellular reabsorption of Ca^{2+} (~25% of filtered load) and Mg^{2+} (~50–70% of filtered load) under the control of the calcium-sensing receptor (CaSR) and a lumen-positive transepithelial voltage. Whereas the proximal Mg^{2+} reabsorption is not altered by dietary intake, the distal tubule matches Mg^{2+} reabsorption to dietary input [23]. The cation-selective paracellular pathway in the TAL primarily depends on the pore formed by claudin-16 and claudin-19 [21], with claudin-14 inhibiting the cation selectivity of that pore [16]. The final handling of Ca^{2+} and Mg^{2+} takes place in the distal convoluted tubule (DCT), where ~10% of the total load is reabsorbed through the cation channels TRPV5 and TRPM6, respectively [6, 7].

Genetic evidence supports the importance of the paracellular pathway components for Ca^{2+} and Mg^{2+} handling by the kidney. Inactivating mutations in the *CLDN16* and *CLDN19* genes coding for claudin-16 and claudin-19, respectively, cause familial hypomagnesemia with hypercalciuria and nephrocalcinosis (FHHNC, OMIM 248250 and 248190), a recessive disease characterized by renal Mg^{2+} and Ca^{2+} wasting, hypomagnesemia, nephrocalcinosis, and progressive renal failure [26, 38]. Mice with knockdown of claudin-16 or claudin-19 showed renal Mg^{2+} and Ca^{2+} wasting [20, 22]. Mutations in *CLDN14* cause rare autosomal recessive nonsyndromic deafness (OMIM 614035), but these patients have apparently normal renal parameters [46]. Genome-wide association studies (GWAS) [40] have revealed a common variant in *CLDN14* (rs219780) associated with an increased risk of kidney stone and reduced bone mineral density, the risk allele being suggestively associated with increased urinary Ca^{2+} excretion. A population-based candidate gene sequencing study identified a *CLDN14* missense variant (rs113831133) associated with 24-h urinary Ca^{2+} excretion [41].

Despite these genetic insights, the paracellular selectivity of the renal tubule for Ca^{2+} and Mg^{2+} remains poorly understood. For instance, inherited disorders of the proximal tubule or the TAL cause hypercalciuria but usually no magnesium wasting [10]. Similarly, the mouse model for Bartter syndrome shows severe hypercalciuria in the absence of renal Mg^{2+} wasting [39]. Also, chronic use of loop diuretics rarely leads to hypomagnesemia, whereas renal Ca^{2+} wasting is a constant finding [5, 34]. Recent studies in vitro and in mouse models support a distinct role of the claudin-16, claudin-19, and claudin-14 in the TAL, where their balance could differentially regulate the permeability for Ca^{2+} and Mg^{2+} [16, 18, 21, 22, 26, 38, 46, 47].

Based on the evidence supporting a differential handling of Ca^{2+} and Mg^{2+}, we hypothesized that using a urinary electrolyte ratio as phenotypic trait (rather than conventional electrolyte normalized over creatinine) could increase the sensitivity to reveal genes involved in specific tubular functions. GWAS on the plasma levels of Ca^{2+} and Mg^{2+} yielded meaningful loci [28, 31], but no GWAS for urinary magnesium-to-calcium ratio is available thus far. To gain novel insights into the genetic determinants of the tubular handling of Ca^{2+} and Mg^{2+}, we conducted a meta-analysis of GWAS for the ratio of urinary Mg^{2+} and Ca^{2+} concentrations (uMg/uCa) in seven cohorts of European descent. The analysis identified a top locus encompassing *CLDN14*, the gene coding for claudin-14. In mouse, we showed that claudin-14 is expressed in the distal

nephron segments specifically handling magnesium and that its expression is regulated by selective changes in the dietary magnesium content. Taken together, these studies support a major role for claudin-14 in the differential paracellular handling of Ca^{2+} and Mg^{2+} by the renal tubule in mammals.

Results

Meta-GWAS for the urinary magnesium over calcium excretion

We conducted a meta-analysis of GWAS for the uMg/uCa ratio in spot urine as a specific phenotype. Seven cohorts of European descent were included, with a total of 9320 samples: Cohorte Lausannoise (CoLaus), CROATIA-Korcula, CROATIA-Split, CROATIA-Vis, the Lothian Birth Cohort 1936 (LBC1936), Network Italiano Isolati Genetici (INGI)-Carlantino, and INGI-Val Borbera. Cohort characteristics are shown in Table 1. The association was performed on a set of ~2.5 M single-nucleotide polymorphisms, both genotyped and imputed based on the HapMap data.

The Manhattan plot on Fig. 1 displays the $-\log_{10}$ (p values) of associations at each locus by chromosomal position. Three association signals show genome-wide significant p values below 5×10^{-8} on chromosomes 1, 5, and 21. Little heterogeneity is present for the three significant associations, only one cohort displaying an opposite effect size, close to null, for the locus on chromosome 1 (Suppl. Fig. 1).

The top signal lies on chromosome 21, in the distal fraction of the gene *CLDN14* (Fig. 2). The top single-nucleotide polymorphism (SNP) (rs172639), harboring an association p value of 1.7×10^{-12}, lies in a noncoding intergenic region, ~28 kb downstream of the three prime untranslated region (3′ UTR) of *CLDN14*. Of note, this SNP is part of a large linkage disequilibrium (LD) block spanning the 3′ *CLDN14* gene region, where two microRNA (miR-374 and miR-9) binding sites have been reported [16]. Furthermore, the four SNPs of *CLDN14* previously associated with kidney stones [40] are included in the same LD block, hence are in LD with rs172639 and also show a high level of association ($p < 10^{-8}$) to the uMg/uCa ratio (Suppl. Fig. S2). The second highest signal lies on chromosome 1 and shows a lowest p value at rs884127 of 3.4×10^{-9}. The locus contains several genes, the closest to the top SNP being *SLC30A10* and *RNU5F-1* (Fig. 3a). A third significantly associated locus is present on chromosome 5, with the lowest p value of 6.3×10^{-9} at the marker rs7447593. This locus harbors multiple genes, the highest association signals being on SNPs lying within the *SLC34A1* gene known to be associated with estimated glomerular filtration rate (eGFR) and chronic kidney disease (CKD) (Fig. 3b). Summary statistics of the associations observed at the three significant loci is detailed on Table 2.

In order to explore to what extent these significant association signals for the uMg/uCa ratio were driven by their association to one of the electrolytes vs. the other, the associations at the three loci were tested with both uMg and uCa concentration, taken individually. For the two top association signals (rs172639 and rs884127), the p value of the association to the uMg/uCa ratio was more significant than each p value of association to the single electrolyte. None of the single electrolyte's association was genome-wide significant on its own. Effect signs observed for each single electrolyte's association were going in opposite directions, explaining the increased significance and the resulting effect sign for the ratio (Table 3).

Tissue and kidney segmental expression of claudin-14 in the mouse

When assessed by RT-qPCR (Fig. 4a), the expression of *Cldn14* messenger RNA (mRNA) was the highest in the mouse liver, followed by the colon, kidney, and brain (inner ears), with very low levels in the stomach and ileum. The transcript was not detected in the duodenum, bone, heart, lung, muscle, and peritoneum (not shown). Based on well-characterized tubular fractions [15], the highest expression level of *Cldn14* was detected in the TAL, together with that of *Cldn16* and *Cldn19* (Fig. 4b). Of note, *Cldn14* transcripts were also weakly detected in the proximal convoluted and straight tubules (PCT and PST; ~25% of TAL expression) and in the distal tubule (DCT and collecting duct, ~75% of TAL expression). The enrichment of *Cldn14* transcripts in the TAL was substantiated by comparing expression levels in total kidney extracts, in primary mouse thick ascending limb (mTAL) cells, and in microdissected TAL tubules (Fig. 4c). Immunofluorescence analysis of rodent kidney sections (Fig. 4d–e) showed substantial co-localization of claudin-14 with uromodulin in TAL profiles. A sizeable amount of claudin-14-positive tubules stained negative for uromodulin. In accordance with our transcript data showing distal enrichment of *Cldn14* expression, we found co-localization of claudin-14 with sodium chloride co-transporter (NCC) and aquaporin-2 (AQP2) in DCT and collecting ducts (CD), respectively.

Effect of dietary magnesium on the expression of claudin-14

In order to substantiate the potential role of claudin-14 in renal tubular handling of Mg^{2+}, mice were randomly assigned to a low Mg^{2+} diet (0.005% *w*/*w* Mg^{2+}), a high Mg^{2+} diet (0.48% *w*/*w* Mg^{2+}), or a control diet (0.19% *w*/*w* Mg^{2+}) for 10 days. These dietary changes induced profound, specific alterations in the renal handling of divalent cations as evidenced by the

Table 1 Summary of participating cohorts' characteristics

Study	CoLaus	INGI-Val Borbera	INGI-Carlantino	CROATIA-Vis	CROATIA-Korcula	CROATIA-Split	LBC1936
Sample size (*N*)	5265	1541	281	195	889	489	660
Female %	53%	56%	57%	58%	64%	56%	48%
Age, years mean (SD)	53.4 (10.7)	55 (18)	48 (19.7)	56.34 (15.5)	56.3 (13.9)	49.2 (14.7)	72.7 (0.75)
Urine Mg (mg/dl) mean (SD)	6.9 (4.0)	8.4 (4.8)	8.1 (5.0)	5.93 (4.52)	7.6 (4)	8.76 (4.9)	8.70 (5.61)
Urine Ca (mg/dl) mean (SD)	10.3 (6.62)	13.0 (10.1)	9.37 (7.54)	9.44 (6.54)	11.6 (7.70)	12.7 (8.94)	11.1 (7.84)
Urine Mg/Ca ratio mean (SD)	0.88 (0.68)	0.93 (1.02)	1.24 (1.03)	0.74 (0.63)	0.92 (0.83)	0.88 (0.59)	1.06 (0.83)
Urine Mg/urinary creatinine (mg/g creat) mean (SD)	46.5 (25.9)	88.6 (36.5)	105 (44.8)	62.5 (33.4)	63.7 (32.5)	60.6 (26.8)	82.0 (42.2)
Urine Ca/urinary creatinine (mg/g creat) mean (SD)	75.1 (57.1)	131.7 (82.6)	123.6 (83.9)	113.4 (97.7)	99.2 (68.1)	92.0 (64.5)	108.8 (73.5)
FEMg mean (SD)	3.27 (1.65)	5.2 (2.5)	6.0 (2.6)	NA	2.55 (1.33)	NA	NA
eGFR mean (SD)	89.4 (20.1)	89.2 (23.3)	NA	89.4 (21.2)	87.7 (21.16)	94.9 (23.3)	NA

FEMg fractional excretion of Mg^{2+}, *eGFR* estimated glomerular filtration rate

uMg/uCa ratio (Fig. 4f, Suppl. Table S2, Suppl. Fig. S3) and induced changes in plasma Mg^{2+} levels (Suppl. Table S3). Of note, urinary excretion of Ca^{2+} was not affected by the different diets here although mice on low Mg^{2+} diet developed hypocalcemia (Suppl. Table S2, S3, Suppl. Fig. S3). The fact that the different Mg^{2+} diets were inducing alterations in renal Mg^{2+} excretion without affecting renal Ca^{2+} excretion suggests specific and probably distal renal regulation mechanisms for these cations. Evaluation of the transcript levels of magnesiotropic and calciotropic genes as well as genes expressed in the TAL (Fig. 4g) revealed specific changes in *Trpm6* encoding epithelial Mg^{2+} channel TRPM6 (133 ± 8% of control expression, $p < 0.01$) and *Trpv5* encoding Ca^{2+} channel TRPV5 (64 ± 7% of control expression, $p < 0.01$) under low Mg^{2+} diet. Of interest, *Cldn14* transcripts were decreased by ~50% under low Mg^{2+} diet, contrasting with

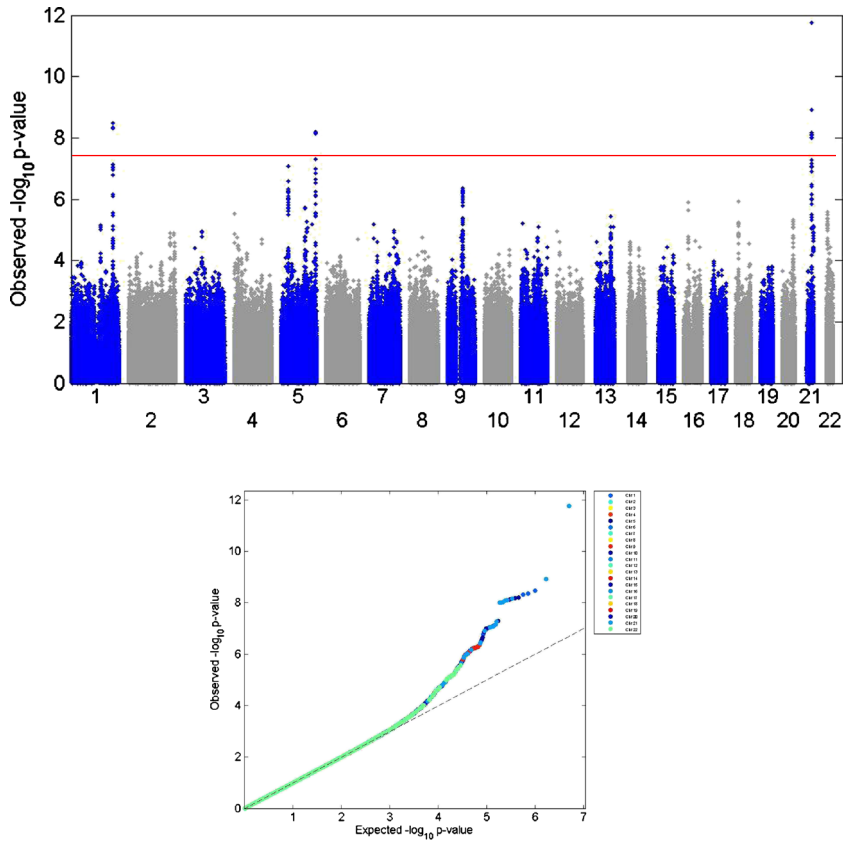

Fig. 1 Manhattan plot and QQ plot of the GWAS for the uMg/uCa ratio. Manhattan plot showing the $-\log_{10}$ (*p* value) (*Y*-axis) of the association seen at each tested marker of the uMg/uCa GWAS (*top panel*). The *X*-axis represents the genetic location, chromosome by chromosome. QQ plot of the GWAS showing inflation with respect to the identity line, evidencing significant association signals (*bottom panel*)

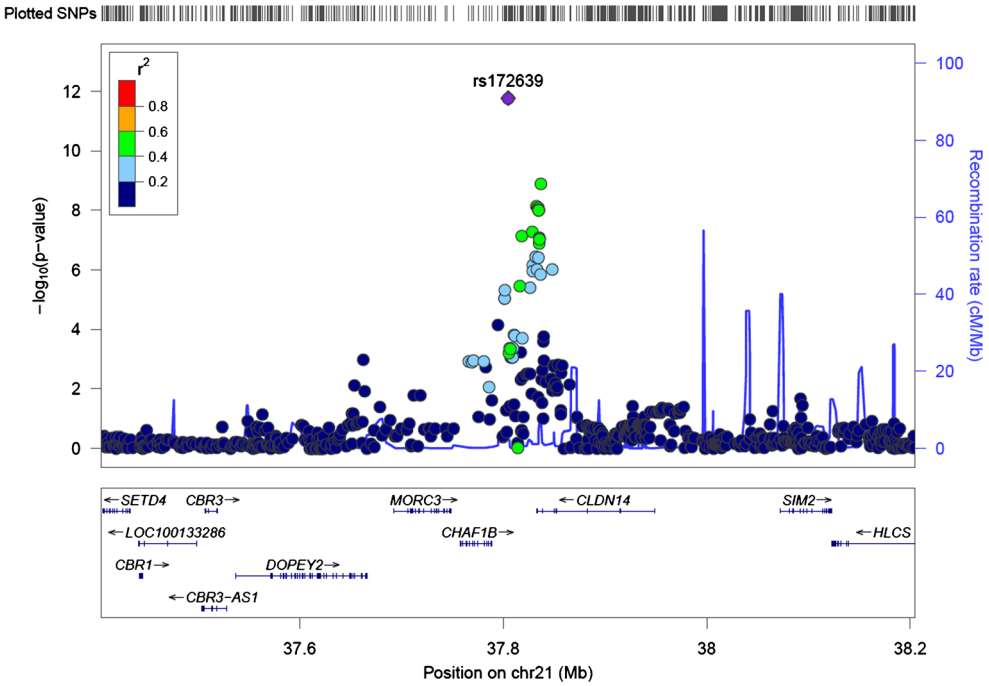

Fig. 2 Regional plot of the rs172639 locus. Zoom of the locus showing the genetic context of it. Each *dot* is one marker; the *color code* refers to the linkage disequilibrium toward the top SNP (represented by a *purple diamond*)

the unchanged expression of *Cldn16* and *Cldn19*. The regulation of *Cldn14* expression by Mg^{2+} intake was specific because other genes expressed in the TAL segment such as *Slc12a1* (NKCC2), *Kcnj1* (ROMK), and *Casr* (calcium-sensing receptor) were not affected. Neither Mg^{2+} supplementation nor Mg^{2+} restriction was inducing changes in CaSR protein expression in the kidney (Suppl. Fig. S3). In contrast, high Mg^{2+} intake increased the expression of claudin-14 in the kidney, as assessed by western blot (Fig. 4h). Taken together, these data reveal that the expression of claudin-14 is specifically influenced by changes in the dietary magnesium content, compatible with the inhibitory role in paracellular Mg^{2+} reabsorption.

Discussion

Our study, this first GWAS on urinary magnesium-to-calcium ratio, found significant associations with three genetic loci to the phenotype using cohorts covering a wide range of environmental as well as cultural settings across Europe. Urinary Ca^{2+} and Mg^{2+} levels were measured in the same central laboratory, thereby minimizing a potential source of noise. The two top signals (rs172639 and rs884127) are specific for the uMg/uCa ratio, since none of the associations to the individual cations are genome-wide significant on their own. The top variant, rs172639 (chromosome 21), suggests the *CLDN14* gene as a plausible candidate for regulating the specific handling of Mg^{2+} and Ca^{2+} by the kidney tubule. The least significantly associated variant (rs7447593) was found to be driven by the underlying association to uCa.

The first and most significantly associated locus is *CLDN14*. The top SNP, rs172639, lies downstream of the 3′ UTR, within a large LD block spanning the 3′ *CLDN14* gene region, where binding sites for miR-374 and miR-9 have been reported [16] and also including the four SNPs previously associated with kidney stones [40]. The prior knowledge of the protein, claudin-14, supports the gene as the best biological candidate. Although the association of rs172639 with uCa (indexed to urinary creatinine) was much more significant than the one with uMg, none of them would have reached genome-wide significance when taken one at a time. The *p* value of the ratio is more than four orders of magnitude lower than the *p* values of each of the electrolytes, thereby highlighting the power of a urinary electrolyte ratio to identify genetic determinants of renal tubular handling.

The second significant association is found at rs884127. The associated SNPs lie in the coding region of two overlapping genes: *SLC30A10* and *RNU5F-1*. Interestingly, none of the association to either of the two electrolytes constituting the ratio would exceed 10^{-3}. Therefore, the association at this locus seems equally driven, although in opposite directions, by the two electrolytes. Interpretation of the biological relevance of genes in this locus is difficult and would require substantial efforts, given that none of the potentially involved genes show evidence of being the true contributing factor. *SLC30A10* belongs to the SLC30 family of genes coding for zinc and manganese transporters [37]. Inactivating mutations in *SLC30A10* have been associated with hypermanganesemia and Mn accumulation in liver and

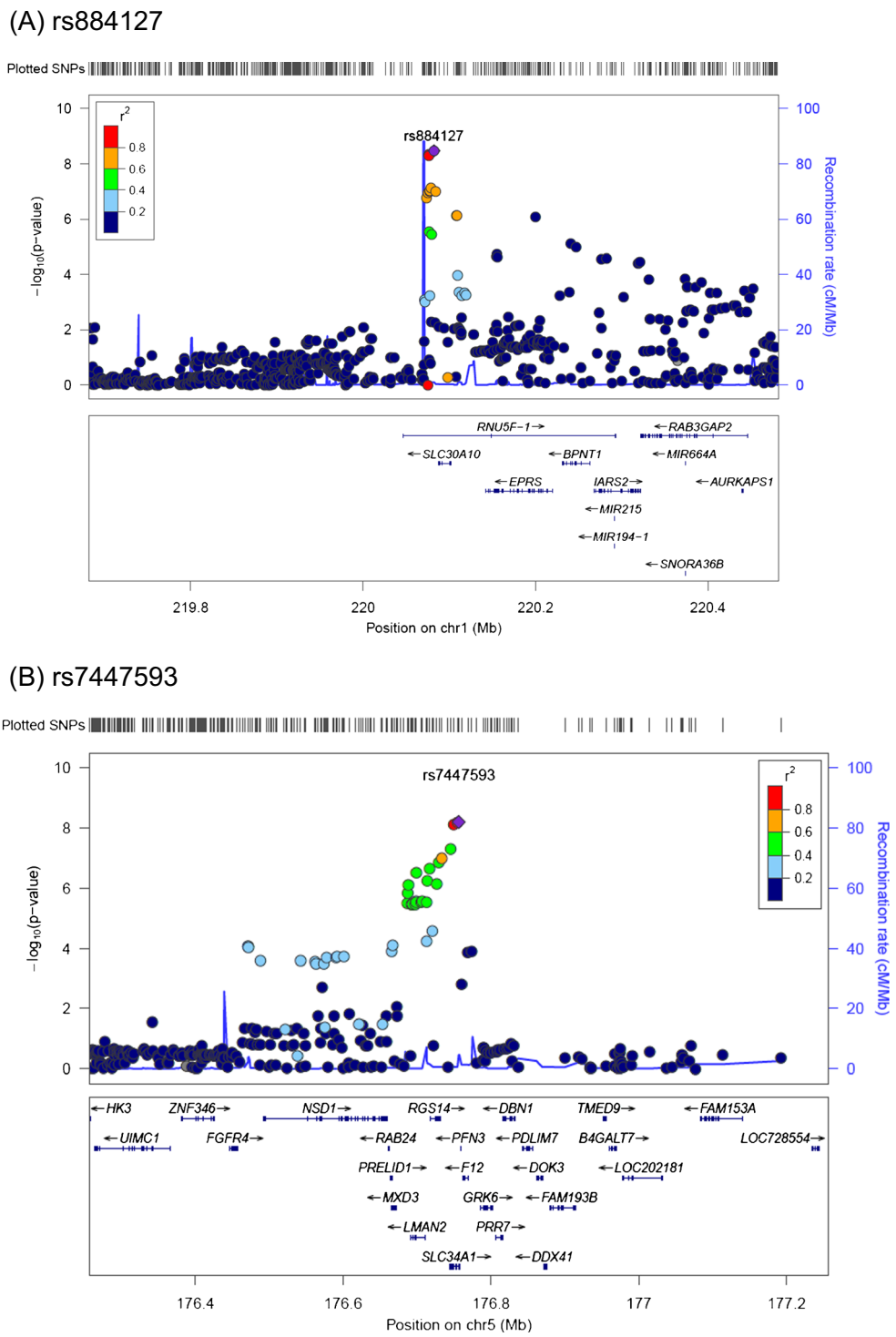

Fig. 3 Regional plots for loci around rs884127 and rs7447593. Zoom of the loci (**a** rs884127 and **b** rs7447593) showing the genetic context of them. Each *dot* is one marker; the *color code* refers to the linkage disequilibrium toward the top SNP (represented by a *purple diamond*)

brain causing hepatic cirrhosis and dystonia [43]. *RNU5F-1* is a snRNA gene, with no evidence for specific role in the kidney.

Based on the robust genetic association, we performed additional studies to address the biological relevance of *CLDN14* in relation to the uMg/uCa ratio. The *Cldn14* mRNA was shown to be highly expressed in the kidney, with transcripts enriched in the TAL, similarly to *Cldn16* and *Cldn19*. Of note, previous reports have shown controversial results regarding *Cldn14* distribution including its expression in proximal tubule segments [1, 13]. Using immunofluorescence, we detected apical claudin-14 signal in tubules positive for uromodulin, supporting the microperfusion studies evidencing the critical role of the TAL for paracellular

Table 2 Summary statistics for the three top SNPs of the loci significantly associated with the uMg/uCa ratio

Chromosome	Position	rs number	Effect allele	Other allele	Mean frequency of the effect allele	Effect	Standard error	Combined *p* value	Direction	I^2
21	36726716	rs172639	c	g	0.4114	0.1139	0.0161	1.71E-12	+++++++	21.6
1	216470545	rs884127	a	g	0.3754	0.0946	0.0160	3.37E-09	+++++−+	0
5	176756743	rs7447593	c	g	0.635	0.1086	0.0187	6.27E-09	+++++++	0

The effect allele has been assigned to the allele increasing the ratio uMg/uCa. The effect is expressed in the transformed scale used to normalize the phenotypes. The sign of the direction of the effect was consistent across all cohorts, except for Carlantino at rs884127 that showed only a moderate effect. The I^2, measure of heterogeneity, shows little to no heterogeneity across cohorts

reabsorption of Mg^{2+} [23]. The relevance of claudin-14 expression in more distal segments (DCT and CD) is less obvious, since no paracellular pathway for Mg^{2+} has been evidenced there.

We showed that claudin-14 expression is regulated by Mg^{2+} intake in mice. Changes in Mg^{2+} diets (with stable Ca^{2+} content) strongly modified the uMg/uCa ratio, the modifications being solely driven by alterations in renal Mg^{2+} excretion. Despite appropriate conservation of Mg^{2+} in the low intake group and Mg^{2+} wasting in the high intake group, mice developed hypomagnesemia and hypermagnesemia, respectively. These changes are reflected by specific variations in kidney transcripts: The low Mg^{2+} diet induces a significant upregulation of *Trpm6* and downregulation of *Trpv5*, confirming that renal adaptation systems are implemented [17, 44]. Of note, the low Mg^{2+} diet induced a strong downregulation of *Cldn14* mRNA, whereas *Cldn16* and *Cldn19* mRNA levels were unchanged. In contrast, others have shown that Ca^{2+} deprivation had no effect on *Cldn14* expression in mouse kidney [12]. Whether the selective reduction of *Cldn14* transcripts is contributing to a greater paracellular uptake of Mg^{2+} in the TAL, for instance by lifting the inhibition of the claudin-16/claudin-19 pore in Mg^{2+} deprivation, remains to be investigated.

The observation that dietary Mg^{2+} loading is leading to increased claudin-14 expression in the kidney is physiologically meaningful. Since claudin-14 blocks the paracellular cation channels made by claudin-16 and claudin-19 [16], a higher claudin-14 expression will lead to reduced paracellular cation uptake and protection from Mg^{2+} overload. In contrast to previous reports [17, 44], we did not detect major changes in renal Ca^{2+} excretion, whereas lowered plasma Ca^{2+} levels in the low Mg^{2+} intake group suggest alterations in intestinal handling of Ca^{2+} or modified bone turnover. Due to technical limitations, we do not have plasma PTH levels, which would be required to study the interrelations of Mg^{2+} and Ca^{2+} homeostasis. At any rate, the upregulation of claudin-14 after high Mg^{2+} diet is unlikely to be triggered by extracellular Ca^{2+} sensing since plasma Ca^{2+} levels were unchanged. Overall, the fact that claudin-14 levels correlate with the uMg/uCa ratio in mouse supports a role for this protein in the differential handling of Ca^{2+} and Mg^{2+} in the distal nephron, complementing the GWAS data.

The association of common variants in *CLDN14* with the uMg/uCa ratio suggests that claudin-14 may interact with the claudin-16/claudin-19 pore, resulting in a differential handling of the two cations. This hypothesis is supported by the specific regulation of the *Cldn14* transcript in the kidney, compared to other claudins or to Mg^{2+} and Ca^{2+} transporters, during changes in magnesium diet. Genetic and pharmacologic conditions targeting the TAL seem to have substantially more consequences on renal Ca^{2+} handling than on Mg^{2+} handling [48]. A few human *CLDN16* mutations were described that led to a phenotype of profound calcium wasting and almost no alterations in Mg^{2+} homeostasis [29]. In vitro, Hou et al. [19] noted that the induction of claudin-16 in LLC-PK1 cells induced a relatively small increase in Mg^{2+} permeability compared to the increase in Na^+ permeability, but Ca^{2+} was not tested. In contrast, it was reported that the expression of claudin-16 in MDCK cells increased the permeability for Mg^{2+} without affecting the ratio P_{Na}/P_{Cl} and increased the apical-to-basolateral permeability for Ca^{2+} [24, 25]. Isolated TALs from

Table 3 Summary statistics for the association at the three loci with the different Mg^{2+} and Ca^{2+} urine traits

SNP	Locus' main gene of interest	Effect allele	uMg/uCa		uMg/ucreatinine		uCa/ucreatinine	
			p value	Effect (SE)	*p* value	Effect (SE)	*p* value	Effect (SE)
rs172639	*CLDN14*	c	1.71E-12	0.1139 (0.0161)	0.3029	0.0162 (0.0158)	6.09E-07	−0.0807 (0.0162)
rs884127	*SLC30A10*	a	3.37E-09	0.0946 (0.0160)	0.008584	0.0412 (0.0157)	0.001004	−0.0527 (0.0160)
rs7447593	*SLC34A1*	c	6.27E-09	0.1086 (0.0187)	0.2363	−0.0219 (0.0185)	8.19E-09	−0.109 (0.0189)

The associations of the three loci are shown for the uMg/uCa ratio, the uMg over urinary creatinine ratio, and uCa over urinary creatinine ratio

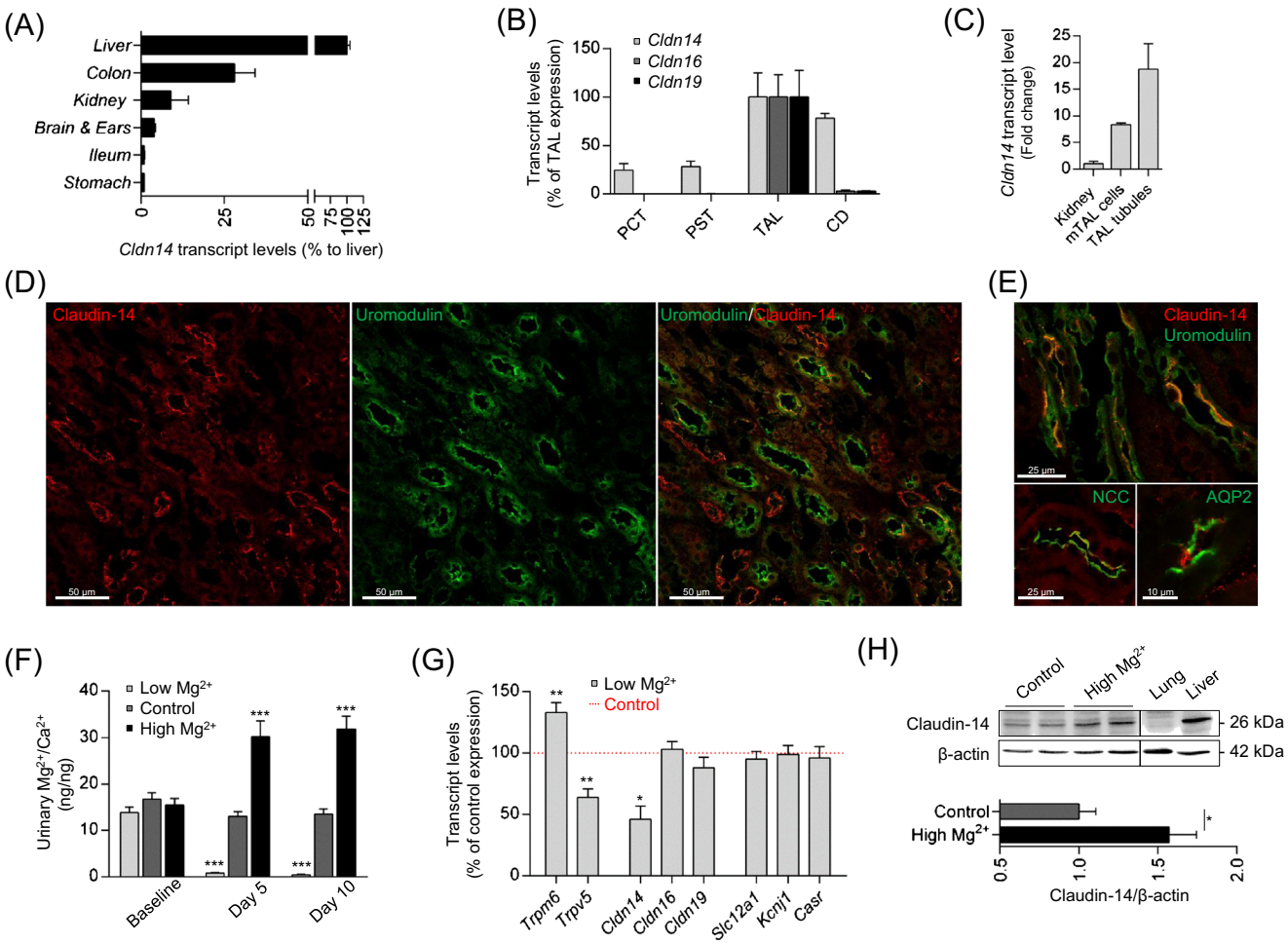

Fig. 4 Expression and regulation of claudin-14 in the kidney. **a** *Cldn14* transcript levels as assessed by RT-qPCR in various mouse tissues. The highest expression was detected in the liver, followed by the colon, kidney, and brain with inner ears. Very weak *Cldn14* expression was detected in stomach and ileum. Transcript levels were normalized to *Gapdh* and expressed relative to liver expression (100%); *bars* indicate means ± SEM; $N = 3$. **b** Transcript levels of *Cldn14*, *Cldn16*, and *Cldn19* along the mouse nephron. Using RT-qPCR on well-characterized tubular fractions [15], the highest expression levels for the three claudins were detected in the thick ascending limb (TAL). *Cldn14* transcripts are also weakly detected in the proximal convoluted and straight tubules (PCT and PST; ~25% of TAL expression) and are enriched in the collecting duct (CD, ~75% of TAL expression), under standard diet conditions. *Bars* indicate means ± SEM; $N = 3$. **c** Enrichment of *Cldn14* transcripts in the TAL as assessed by RT-qPCR on total kidney extracts, on primary mouse thick ascending limb (mTAL) cells, and on microdissected TAL tubules. After normalization to *Gapdh*, and compared to total kidney, *Cldn14* transcripts are ~8× more abundant in mTAL cells and ~18× higher in microdissected TAL tubules. *Bars* indicate means ± SEM; $N = 3$. **d** Immunofluorescence analysis of rat (under high Mg^{2+} diet) kidney section showing partial co-distribution of claudin-14 (*red*) with uromodulin (*green*). A subset of claudin-14-positive tubules stained negative for uromodulin. Claudin-14 shows an apical staining pattern, co-localizing with uromodulin on the apical membrane (*yellow staining* on merged picture). **e** Higher magnification immunofluorescence analysis of claudin-14 (*red* in all sections) co-distribution with uromodulin, NCC, or AQP2 (as indicated, in *green*). Claudin-14-positive tubules were found positive for uromodulin, NCC, and AQP2, confirming the RT-qPCR data of distal tubular distribution of claudin-14 expression. **f** Age-matched C57BL/6J mice were assigned to a low Mg^{2+} diet (0.005% *w/w* Mg^{2+}), a high Mg^{2+} diet (0.48% *w/w* Mg^{2+}), or a control diet (0.19% *w/w* Mg^{2+}) for 10 days. Urinary Mg^{2+} over Ca^{2+} excretion ratios (ng/ng) are depicted before (baseline) and after 5 and 10 days on the respective diets. Profound alterations in the ratio of urinary Mg^{2+}/Ca^{2+} excretion are detected after 5 days on the respective diets and are maintained on day 10. *Bars* indicate means ± SEM; N = 7–17; $^{***}p < 0.001$ compared to control diet. **g** Kidney transcript levels of magnesiotropic and calciotropic genes as well as genes expressed in the TAL after low Mg^{2+} diet, as assessed by RT-qPCR. Expression levels of *Trpm6* encoding epithelial Mg^{2+} channel TRPM6 were increased, and expression levels of *Trpv5* encoding Ca^{2+} channel TRPV5 were decreased after 10 days of low Mg^{2+} diet. Of interest, *Cldn14* transcripts were decreased by ~50% after 10 days of low Mg^{2+} diet, but expression of *Cldn16* and *Cldn19* was not altered. Regulation of *Cldn14* expression by Mg^{2+} intake was specific because other genes expressed in the TAL segment such as *Slc12a1*, *Kcnj1*, and *Casr* were not affected. *Bars* indicate means ± SEM; N = at least 4; $^{*}p < 0.05$, $^{**}p < 0.01$ compared to control diet. **h** Representative western blot showing the increase of claudin-14 protein levels in total kidney extracts after 10 days of high Mg^{2+} diet. Total protein extracts from liver and lung were loaded as positive and negative controls, respectively, and were run on the same blot. β-Actin is shown as a loading control. Densitometric analysis of claudin-14 signal normalized to β-actin is shown below the blots. *Bars* indicate means ± SEM; $N = 3$; $^{*}p < 0.05$

Cldn16 knockdown animals showed a primary defect in the selective permeability for Na^+ without effects on P_{Mg} [20], whereas P_{Mg}/P_{Na} and P_{Ca}/P_{Na} ratios were equally reduced in TALs from *Cldn16*$^{-/-}$ mice [47]. Further work, e.g., based on microperfusion, is needed to delineate the paracellular permeability ratios for Mg^{2+} and Ca^{2+} in the TAL. Also, we cannot exclude that the paracellular handling for Mg^{2+} and Ca^{2+} is similarly affected by variants in *CLDN14* but that adaptation mechanisms in more distal segments are more efficient in conserving either Mg^{2+} or Ca^{2+} [4]. Molecular switches that regulate the mass and function of the DCT with profound effect on renal Ca^{2+} and Mg^{2+} handling have been previously described [27]. Furthermore, low Mg^{2+} diet in mice resulted in opposite effects on the transcript levels of distal tubule Ca^{2+} and Mg^{2+} channels (TRPV5 and TRPM6, respectively).

Our findings confirm the value of dietary experiments in mouse models to functionally explore GWAS results in humans. In a prior GWAS on serum calcium, the identified genes were differentially expressed in the bone, but not in the kidney, in response to changes in dietary Ca^{2+} intake in mice [31]. It seems reasonable to postulate that dietary changes in humans would lead to similar gene expression and physiologic responses to those observed in mice. Hence, if one accepts the value of urinary electrolytes as nutrition biomarkers in humans, GWAS on urinary phenotypes represent a powerful tool in the field of nutrigenomics.

In the context of the recent GWAS finding showing that variants in *CLDN14* were associated with the risk of kidney stones [40] and the present work linking *CLDN14* to the urinary excretion ratio of Mg^{2+} over Ca^{2+}, it is interesting to note that the first-degree relatives of FHHNC patients (mutations in *CLDN16/19*) present a clear trend for hypercalciuria with renal stones and hypomagnesemia [2, 33]. These observations support that genetic defects in claudins expressed in the TAL are part of a spectrum including common complex traits and rare mendelian disorders, as already observed for other genes involved in tubular disorders [11].

Material and methods

Cohorts Seven European cohorts participated in the study. The largest is CoLaus, a population-based cohort from Switzerland with baseline examination conducted between 2003 and 2006. It includes 6184 individuals of European descent aged 35–75 years randomly selected from the registry of the city of Lausanne [14]. The CROATIA-Vis study, Croatia, is a family-based, cross-sectional study in the isolated island of Vis that included 1056 examinees aged 18–93 years. Blood samples were collected in 2003 and 2004 [45]. The CROATIA-Korcula study, Croatia, is a family-based, cross-sectional study in the isolated island of Korcula that included 965 examinees aged 18–95. Blood samples were collected in 2007 [32]. The CROATIA-Split study, Croatia, is a population-based, cross-sectional study in the Dalmatian city of Split that so far includes 1012 examinees aged 18–95. Blood samples were collected in 2009–2011 [36]. The Lothian Birth Cohort 1936 (LBC1936) consists of 1091 relatively healthy older participants, most of whom took part in the Scottish Mental Survey of 1947 at the age of about 11 years. At a mean age of 69.5 years (SD 0.8), they were recruited in a study investigating influences on cognitive aging [8]. A second wave of cognitive and physical testing occurred at approximately 73 years of age at which time a urine sample was collected [8, 9]. The INGI-Val Borbera population includes 1785 genotyped samples (18–102 years) collected in the Val Borbera Valley, a geographically isolated valley located within the Appennine Mountains in Northwest Italy [42]. The INGI-Carlantino study is a population-based, cross-sectional study in a village situated in the southeastern part of the Apennines in a hilly area of the Puglia region. The main study characteristics are summarized in Table 1, genotyping details on Suppl. Table S1.

Laboratory measurements Electrolytes, hematology parameters, and glycemia were measured in the university laboratories in Zürich using standard clinical laboratory methods. Creatinine was measured using Jaffe kinetic compensated method (Roche Diagnostics, Switzerland, intra-assay variability 0.7–2.9%). The CKD-EPI formula was used to calculate the eGFR. All urinary biochemical parameters were measured from samples stored at −80 °C, using the same biochemical platform UniCel® DxC 800 Synchron® Clinical System (Beckman Coulter, Nyon, Switzerland) at the University of Zürich. Appropriate controls and sets of calibration standards were used before running each sample batch. All cohorts were subjected to the same measurement protocol, in the same laboratory.

Microdissection of renal tubules Isolation of mouse tubular fractions was performed as previously described [15]. In brief, the kidneys from male C57BL/6J mice were dissected and cut in small pieces before incubation in a HBSS-based dissection solution supplemented with 245 U/ml type 2 collagenase (Worthington Biochemical Corp., Lakewood, NJ) and 96 μg/ml soybean trypsin inhibitor (Sigma-Aldrich, Saint-Louis, MO) for 30 min at 37 °C. Digested tissues were then thieved through a 250-μm filter and retained on a 50-μm filter (Sefar AG, Thal, Switzerland) and collected in dissection solution supplemented with 1% (*w*/*v*) BSA (Sigma-Aldrich). Distinct tubular segments (PCT, PST, TAL, and CD) were identified upon their morphologic features and manually collected. Three distinct collections (~75 tubules each) from each tubular fraction were snap-frozen in liquid nitrogen and conserved at −80 °C.

Primary cell culture Primary mouse thick ascending limb cell cultures are obtained by seeding TALs on collagen-coated 0.33-cm^2 PTFE filter membranes (Transwell-COL, pore size 0.4 μm, Corning Inc., Corning, NY). The generation and characterization of mTAL primary cell cultures were previously described [15].

Gene expression analysis Total RNA was extracted from tissues and microdissected tubules using Aurum TM Total RNA Fatty and Fibrous Tissue Kit (Bio-Rad, Hercules, CA) and RNAqueous-Micro (Ambion, Huntingdon, UK), respectively, following the manufacturer's protocol. DNAse I treatment was performed to eliminate genomic DNA contamination. Reverse transcriptase PCR was performed with iScript TM cDNA Synthesis Kit (Bio-Rad). Relative mRNA levels were determined by RT-qPCR with a CFX96TM Real-Time PCR Detection System (Bio-Rad) using iQ TM SYBR Green Supermix (Bio-Rad). Specific primers were designed using Primer3 [35], and the efficiency of each set of primers was determined by dilution curves (Suppl. Table S4). The PCR products were sequenced with the BigDye Terminator Kit (Perkin Elmer Applied Biosystems, Waltham, MA). The MultiScreen SEQ384 Filter Plate (Millipore, Billerica, MA) and Sephadex G-50 DNA Grade Fine (Amersham Biosciences, Piscataway, NJ) dye terminator removal were used to purify sequence reactions before analysis on an ABI3100 capillary sequencer (PerkinElmer Applied Biosystems).

Mouse studies Experiments were performed on age-matched and gender-matched C57BL/6J littermates. Mice were housed in a temperature-controlled and light-controlled room with ad libitum access to standard pellet chow (SSNIFF Spezialdiäten, Soest, Germany) and deionized drinking water for 4 weeks until the start of the experiment. Three groups of mice were next fed a control diet (0.19% *w*/*w* Mg^{2+}, $n = 20$), a Mg^{2+}-deficient diet (0.005% *w*/*w* Mg^{2+}, $n = 22$), or a Mg^{2+}-enriched diet (0.48% *w*/*w* Mg^{2+}, $n = 20$) (SSNIFF Spezialdiäten) for 10 days. The Ca^{2+} content was kept constant (0.9% *w*/*w*) in the three diets. Mice were housed individually in metabolic cages before, at day 5, and at day 10 for overnight urine collection (16-h sampling). Urinary and plasma electrolytes were measured on a Synchron Unicel DxC 800 analyzer (Beckman Coulter, Brea, CA). Plasma urea was determined using the Synchron CX®3 Delta System (Beckman Coulter), and plasma creatinine was measured by enzymatic reaction (Beckman Coulter). The kidneys for immunostaining and immunoblotting were harvested at day 10 and snap-frozen in liquid nitrogen. All protocols were conducted in accordance with the National Research Council Guide for the Care and Use of Laboratory animals and were approved by the Ethics Committee of the Université catholique de Louvain.

Immunoblotting Tissues were homogenized by using a pestle and mortar and solubilized in ice-cold RIPA buffer (Sigma-Aldrich) supplemented with protease inhibitors (cOmplete Mini, Roche, Basel, Switzerland), followed by a centrifugation for 15 min at 1000×*g*, 4 °C, and a brief sonication of the supernatant. Protein concentration in lysates was quantified using the bicinchoninic acid (BCA) protein assay kit (Thermo Fischer Scientific, Waltham, MA). Lysates were mixed with Laemmli sample buffer (Bio-Rad). Proteins were separated on an SDS-PAGE gel in reducing conditions and transferred onto PVDF membrane (Bio-Rad). Western blotting was performed using established protocols [15]. Goat polyclonal anti-claudin-14 antibodies (sc-47842, Santa Cruz Biotechnology, Dallas, TX; 1:250), mouse monoclonal anti-CaSR antibody (MA1-934, Thermo Fischer Scientific; 1:500), or mouse monoclonal anti-β-actin antibody (A5441, Sigma-Aldrich; 1:10,000) were used as primary antibodies followed by incubation with appropriated peroxidase-conjugated secondary antibodies (Dako, Glostrup, Denmark). Densitometric quantification was done with the ImageJ software (Image Processing Program, NIH, USA).

Immunofluorescence The kidneys from rat and mice-fed Mg^{2+}-rich diet were fixed with 2–4% PFA in PBS and embedded in O.C.T compound or paraffin, respectively. Eight micrometer thick kidney sections were incubated in 100% methanol for 20 min at −20 °C; then, antigen retrieval was performed in a 10 mM citric acid solution (pH 6.0) at 98 °C for 10 min in a tissue processor (Histos Pro, Milestone Inc., Shelton, CT). Sections were then blocked in PBS (Thermo Fischer Scientific) containing 3% BSA (Sigma-Aldrich), 30 mM glycine (Sigma-Aldrich), 50 mM NH_4Cl (VWR International, Radnor, PA), and 0.05% Tween-20 (Millipore) for 1 h at room temperature. Samples were incubated with anti-claudin-14 rabbit antibodies (1:1000, gift from Jianghui Hou, Washington University School of Medicine) or polyclonal anti-claudin-14 antibodies (sc-47842, Santa Cruz Biotechnology, Dallas, TX; 1:50) overnight at 4 °C and subsequently with the appropriated AlexaFluor-labeled secondary antibody (Life Technologies, Carlsbad, CA; 1:1000) for 1 h at room temperature. For double-labeling immunofluorescence, sections were incubated with sheep anti-uromodulin antibody (Meridian Life Science, Memphis, TN; 1:300), rabbit anti-NCC antibody (AB 3553, Millipore; 1:300), or rabbit anti-AQP2 antibody (SAB2106671; Sigma-Aldrich; 1:300) for 2 h at room temperature followed by washing and incubation with appropriated AlexaFluor-labeled secondary antibody (Life Technologies; 1:1000). Kidney sections were mounted in Prolong Gold anti-fade reagent containing DAPI (Invitrogen Corp., Waltham, MA) and viewed under a confocal microscope (TCS SP8, Leica Microsystems GmbH, Wetzlar, Germany) using a ×63 1.4 NA oil immersion objective.

Statistical analysis For each cohort, a GWAS was performed on about 2.5 M genotyped and imputed SNPs, by applying a linear regression and an additive genetic model. The trait (uMg/uCa) was transformed by a QQ normalization to fit normality and adjusted by age and sex. When needed, the data were adjusted by study center, relatedness, or any stratification by using the three of four first genotype's principal components. The meta-analysis was performed centrally using METAL, applying the inverse variant weighted fixed-effects model. p values were controlled by genomic control at the study and at the meta-analysis levels. The p values below 5×10^{-8} were considered genome-wide significant. Rare SNPs (<1%) and poorly imputed ($R^2 < 0.3$) SNPs were excluded from the study. For animal studies, values are expressed as means ± standard error of the mean (SEM). Statistical comparisons were performed using a two-tailed unpaired Student's t test (Microsoft Excel, Redmond, WA). p-values <0.05 were considered as statistically significant.

Acknowledgements The CoLaus study is supported by research grants from GlaxoSmithKline, the Faculty of Biology and Medicine of Lausanne, and the Swiss National Science Foundation (grants 33CSCO-122661, 33CS30-139468, and 33CS30-148401). The computations for CoLaus imputation were performed in part at the Vital-IT Center for high performance computing of the Swiss Institute of Bioinformatics. MBO and TC are supported by the Swiss National Centre of Competence in Research Kidney Control of Homeostasis (NCCR Kidney.CH) program. OD is supported by grants from the European Community's Seventh Framework Program (305608 EURenOmics), the Swiss National Centre of Competence in Research Kidney Control of Homeostasis (NCCR Kidney.CH) program, the Swiss National Science Foundation (310030-146490), and the Rare Disease Initiative Zurich (radiz), a clinical research priority program of the University of Zurich, Switzerland. EO is supported by the Fonds National de la Recherche Luxembourg (6903109) and the University Research Priority Program "Integrative Human Physiology, ZIHP" of the University of Zurich. NT is supported by funding from Swiss National Science Foundation Early and Advanced PostdocMolibity Fellowship (P2LAP3_151782 and P300P3_158521).

The CROATIA-Korcula and CROATIA-Split studies were funded by grants from the Medical Research Council (UK), European Commission Framework 6 project EUROSPAN (Contract No. LSHG-CT-2006-018947), and Republic of Croatia Ministry of Science, Education, and Sports research grants to IR (108-1080315-0302). We would like to acknowledge the invaluable contributions of the recruitment team in Korcula and Split, the administrative teams in Croatia and Edinburgh, and the people of Korcula and Split.

The SNP genotyping for the CROATIA-Korcula cohort was performed in Helmholtz Zentrum München, Neuherberg, Germany. The SNP genotyping for the CROATIA-Split cohort was performed by AROS Applied Biotechnology, Aarhus, Denmark.

INGI-Carlantino: We thank Anna Morgan and Angela D'Eustacchio for technical support. We are very grateful to the municipal administrators for their collaboration on the project and for logistic support. We would like to thank all participants to this study.

For the INGI-VALBORBERA study, the research was supported by funds from Compagnia di San Paolo, Torino, Italy; Fondazione Cariplo, Italy; and Ministry of Health, Ricerca Finalizzata 2008 to DT.

Phenotype collection in the Lothian Birth Cohort 1936 (LBC1936) was supported by Age UK (The Disconnected Mind project). Genotyping was funded by the BBSRC (BB/F019394/1). The work was undertaken by The University of Edinburgh Centre for Cognitive Aging and Cognitive Epidemiology, part of the cross council Lifelong Health and Wellbeing Initiative (MR/K026992/1). Funding from the BBSRC and Medical Research Council (MRC) is gratefully acknowledged. We thank the LBC1936 participants, the LBC1936 team for data collection and collation, and the staff at the Wellcome Trust Clinical Research Facility for bio-sample collection and genotyping.

Other funding sources: European Community's Seventh Framework Program (FP7/2007–2013) under grant agreement no. 246539 (Marie Curie) and grant no. 305608 (EURenOmics), the NCCR Kidney.CH program (Swiss National Science Foundation), the Gebert Rüf Stiftung (Project GRS-038/12), and the Swiss National Science Foundation 310030-146490.

The authors acknowledge Nadine Nägele and Julien Weber for their help with the Platform of Biochemical Analyses at the University of Zurich and thank Jianghui Hou for the anti-claudin-14 antibodies and François Seghers, Yvette Cnops and Sébastien Druart (UCL Brussels) for help with the Mg^{2+} diets.

Compliance with ethical standards

Conflict of interest The authors declare they have no conflict of interest.

References

1. Ben-Yosef T, Belyantseva IA, Saunders TL, Hughes ED, Kawamoto K, Van Itallie CM, Beyer LA, Halsey K, Gardner DJ, Wilcox ER, Rasmussen J, Anderson JM, Dolan DF, Forge A, Raphael Y, Camper SA, Friedman TB (2003) Claudin 14 knockout mice, a model for autosomal recessive deafness DFNB29, are deaf due to cochlear hair cell degeneration. Hum Mol Genet 12:2049–2061. doi:10.1093/hmg/ddg210
2. Blanchard A, Jeunemaitre X, Coudol P, Dechaux M, Froissart M, May A, Demontis R, Fournier A, Paillard M, Houillier P (2001) Paracellin-1 is critical for magnesium and calcium reabsorption in the human thick ascending limb of Henle. Kidney Int 59:2206–2215. doi:10.1046/j.1523-1755.2001.0590062206.x
3. Bleich M, Shan Q, Himmerkus N (2012) Calcium regulation of tight junction permeability. Ann N Y Acad Sci 1258:93–99. doi:10.1111/j.1749-6632.2012.06539.x
4. Bonny O, Rubin A, Huang C-L, Frawley WH, Pak CYC, Moe OW (2008) Mechanism of urinary calcium regulation by urinary magnesium and pH. J Am Soc Nephrol 19:1530–1537. doi:10.1681/ASN.2007091038
5. Bushinsky DA, Favus MJ, Langman CB, Coe FL (1986) Mechanism of chronic hypercalciuria with furosemide: increased calcium absorption. Am J Phys 251:F17–F24
6. De Baaij JHF, Hoenderop JGJ, Bindels RJM (2015) Magnesium in man: implications for health and disease. Physiol Rev 95:1–46. doi:10.1152/physrev.00012.2014
7. De Groot T, Bindels RJM, Hoenderop JGJ (2008) TRPV5: an ingeniously controlled calcium channel. Kidney Int 74:1241–1246. doi:10.1038/ki.2008.320
8. Deary IJ, Gow AJ, Taylor MD, Corley J, Brett C, Wilson V, Campbell H, Whalley LJ, Visscher PM, Porteous DJ, Starr JM (2007) The Lothian birth cohort 1936: a study to examine influences on cognitive ageing from age 11 to age 70 and beyond. BMC Geriatr 7:28. doi:10.1186/1471-2318-7-28
9. Deary IJ, Gow AJ, Pattie A, Starr JM (2012) Cohort profile: the lothian birth cohorts of 1921 and 1936. Int J Epidemiol 41:1576–1584. doi:10.1093/ije/dyr197

10. Devuyst O, Pirson Y (2007) Genetics of hypercalciuric stone forming diseases. Kidney Int 72:1065–1072. doi:10.1038/sj.ki.5002441
11. Devuyst O, Knoers NVAM, Remuzzi G, Schaefer F (2014) Rare inherited kidney diseases: challenges, opportunities, and perspectives. Lancet 383:1844–1859. doi:10.1016/S0140-6736(14)60659-0
12. Dimke H, Desai P, Borovac J, Lau A, Pan W, Alexander RT (2013) Activation of the Ca(2+)-sensing receptor increases renal claudin-14 expression and urinary Ca(2+) excretion. Am J Physiol Renal Physiol 304:F761–F769. doi:10.1152/ajprenal.00263.2012
13. Elkouby-Naor L, Abassi Z, Lagziel A, Gow A, Ben-Yosef T (2008) Double gene deletion reveals lack of cooperation between claudin 11 and claudin 14 tight junction proteins. Cell Tissue Res 333:427–438. doi:10.1007/s00441-008-0621-9
14. Firmann M, Mayor V, Vidal PM, Bochud M, Pécoud A, Hayoz D, Paccaud F, Preisig M, Song KS, Yuan X, Danoff TM, Stirnadel HA, Waterworth D, Mooser V, Waeber G, Vollenweider P (2008) The CoLaus study: a population-based study to investigate the epidemiology and genetic determinants of cardiovascular risk factors and metabolic syndrome. BMC Cardiovasc Disord 8:6. doi:10.1186/1471-2261-8-6
15. Glaudemans B, Terryn S, Gölz N, Brunati M, Cattaneo A, Bachi A, Al-Qusairi L, Ziegler U, Staub O, Rampoldi L, Devuyst O (2014) A primary culture system of mouse thick ascending limb cells with preserved function and uromodulin processing. Pflugers Arch 466:343–356. doi:10.1007/s00424-013-1321-1
16. Gong Y, Renigunta V, Himmerkus N, Zhang J, Renigunta A, Bleich M, Hou J (2012) Claudin-14 regulates renal Ca^{++} transport in response to CaSR signalling via a novel microRNA pathway. EMBO J 31:1999–2012. doi:10.1038/emboj.2012.49
17. Groenestege WMT (2006) The epithelial Mg2+ channel transient receptor potential Melastatin 6 is regulated by dietary Mg2+ content and estrogens. J Am Soc Nephrol 17:1035–1043. doi:10.1681/ASN.2005070700
18. Himmerkus N, Shan Q, Goerke B, Hou J, Goodenough DA, Bleich M (2008) Salt and acid-base metabolism in claudin-16 knockdown mice: impact for the pathophysiology of FHHNC patients. Am J Physiol Renal Physiol 295:F1641–F1647. doi:10.1152/ajprenal.90388.2008
19. Hou J, Paul DL, Goodenough DA (2005) Paracellin-1 and the modulation of ion selectivity of tight junctions. J Cell Sci 118:5109–5118. doi:10.1242/jcs.02631
20. Hou J, Shan Q, Wang T, Gomes AS, Yan Q, Paul DL, Bleich M, Goodenough DA (2007) Transgenic RNAi depletion of claudin-16 and the renal handling of magnesium. J Biol Chem. doi:10.1074/jbc.M700632200
21. Hou J, Renigunta A, Konrad M, Gomes A, Schneeberger E, Paul D, Goodenough DA (2008) Claudin-16 and claudin-19 interact and form a cation-selective tight junction complex. J Clin Invest 118:619–628. doi:10.1172/JCI33970DS1
22. Hou J, Renigunta A, Gomes AS, Hou M, Paul DL, Waldegger S, Goodenough DA (2009) Claudin-16 and claudin-19 interaction is required for their assembly into tight junctions and for renal reabsorption of magnesium. Proc Natl Acad Sci U S A 106:15350–15355. doi:10.1073/pnas.0907724106
23. Houillier P (2014) Mechanisms and regulation of renal magnesium transport. Annu Rev Physiol 76:411–430. doi:10.1146/annurev-physiol-021113-170336
24. Ikari A, Hirai N, Shiroma M, Harada H, Sakai H, Hayashi H, Suzuki Y, Degawa M, Takagi K (2004) Association of paracellin-1 with ZO-1 augments the reabsorption of divalent cations in renal epithelial cells. J Biol Chem 279:54826–54832. doi:10.1074/jbc.M406331200
25. Jaya Kausalya P, Amasheh S, Günzel D, Wurps H, Müller D, Fromm M, Hunziker W (2006) Disease-associated mutations affect intracellular traffic and paracellular Mg^{2+} transport function of claudin-16. J Clin Invest 116:878–891. doi:10.1172/JCI26323
26. Konrad M, Schaller A, Seelow D, Pandey AV, Waldegger S, Lesslauer A, Vitzthum H, Suzuki Y, Luk JM, Becker C, Schlingmann KP, Schmid M, Rodriguez-Soriano J, Ariceta G, Cano F, Enriquez R, Juppner H, Bakkaloglu SA, Hediger MA, Gallati S, Neuhauss SCF, Nurnberg P, Weber S (2006) Mutations in the tight-junction gene claudin 19 (CLDN19) are associated with renal magnesium wasting, renal failure, and severe ocular involvement. Am J Hum Genet 79:949–957. doi:10.1086/508617
27. Lalioti MD, Zhang J, Volkman HM, Kahle KT, Hoffmann KE, Toka HR, Nelson-Williams C, Ellison DH, Flavell R, Booth CJ, Lu Y, Geller DS, Lifton RP (2006) Wnk4 controls blood pressure and potassium homeostasis via regulation of mass and activity of the distal convoluted tubule. Nat Genet 38:1124–1132. doi:10.1038/ng1877
28. Meyer TE, Verwoert GC, Hwang SJ, Glazer NL, Smith AV, van Rooij FJA, Ehret GB, Boerwinkle E, Felix JF, Leak TS, Harris TB, Yang Q, Dehghan A, Aspelund T, Katz R, Homuth G, Kocher T, Rettig R, Ried JS, Gieger C, Prucha H, Pfeufer A, Meitinger T, Coresh J, Hofman A, Sarnak MJ, Chen YDI, Uitterlinden AG, Chakravarti A, Psaty BM, van Duijn CM, Linda-Kao WH, Witteman JCM, Gudnason V, Siscovick DS, Fox CS, Köttgen A (2010) Genome-wide association studies of serum magnesium, potassium, and sodium concentrations identify six loci influencing serum magnesium levels. PLoS Genet. doi:10.1371/journal.pgen.1001045
29. Müller D, Kausalya PJ, Claverie-Martin F, Meij IC, Eggert P, Garcia-Nieto V, Hunziker W (2003) A novel claudin 16 mutation associated with childhood hypercalciuria abolishes binding to ZO-1 and results in lysosomal mistargeting. Am J Hum Genet 73:1293–1301. doi:10.1086/380418
30. Muto S, Hata M, Taniguchi J, Tsuruoka S, Moriwaki K, Saitou M, Furuse K, Sasaki H, Fujimura A, Imai M, Kusano E, Tsukita S, Furuse M (2010) Claudin-2-deficient mice are defective in the leaky and cation-selective paracellular permeability properties of renal proximal tubules. Proc Natl Acad Sci U S A 107:8011–8016. doi:10.1073/pnas.0912901107
31. O'Seaghdha CM, Wu H, Yang Q, Kapur K, Guessous I, Zuber AM, Köttgen A, Stoudmann C, Teumer A, Kutalik Z, Mangino M, Dehghan A, Zhang W, Eiriksdottir G, Li G, Tanaka T, Portas L, Lopez LM, Hayward C, Lohman K, Matsuda K, Padmanabhan S, Firsov D, Sorice R, Ulivi S, Brockhaus AC, Kleber ME, Mahajan A, Ernst FD, Gudnason V, Launer LJ, Mace A, Boerwinckle E, Arking DE, Tanikawa C, Nakamura Y, Brown MJ, Gaspoz JM, Theler JM, Siscovick DS, Psaty BM, Bergmann S, Vollenweider P, Vitart V, Wright AF, Zemunik T, Boban M, Kolcic I, Navarro P, Brown EM, Estrada K, Ding J, Harris TB, Bandinelli S, Hernandez D, Singleton AB, Girotto G, Ruggiero D, d'Adamo AP, Robino A, Meitinger T, Meisinger C, Davies G, Starr JM, Chambers JC, Boehm BO, Winkelmann BR, Huang J, Murgia F, Wild SH, Campbell H, Morris AP, Franco OH, Hofman A, Uitterlinden AG, Rivadeneira F, Völker U, Hannemann A, Biffar R, Hoffmann W, Shin SY, Lescuyer P, Henry H, Schurmann C, Munroe PB, Gasparini P, Pirastu N, Ciullo M, Gieger C, März W, Lind L, Spector TD, Smith AV, Rudan I, Wilson JF, Polasek O, Deary IJ, Pirastu M, Ferrucci L, Liu Y, Kestenbaum B, Kooner JS, Witteman JCM, Nauck M, Kao WHL, Wallaschofski H, Bonny O, Fox CS, Bochud M (2013) Meta-analysis of genome-wide association studies identifies six new loci for serum calcium concentrations. PLoS Genet. doi:10.1371/journal.pgen.1003796
32. Polašek O, Marušić A, Rotim K, Hayward C, Vitart V, Huffman J, Campbell S, Janković S, Boban M, Biloglav Z, Kolčić I, Krželj V, Terzić J, Matec L, Tometić G, Nonković D, Ninčević J, Pehlić M, Žedelj J, Velagić V, Juričić D, Kirac I, Belak Kovačević S, Wright AF, Campbell H, Rudan I (2009) Genome-wide association study

of anthropometric traits in Korčula Island, Croatia. Croat Med J 50: 7–16. doi:10.3325/cmj.2009.50.7

33. Praga M, Vara J, González-Parra E, Andrés A, Alamo C, Araque A, Ortiz A, Rodicio JL (1995) Familial hypomagnesemia with hypercalciuria and nephrocalcinosis. Kidney Int 47:1419–1425. doi:10.1038/ki.1995.199
34. Quamme GA (1997) Renal magnesium handling: new insights in understanding old problems. Kidney Int 52:1180–1195. doi:10.1038/ki.1997.443
35. Rozen S, Skaletsky H (2000) Primer3 on the WWW for general users and for biologist programmers. Methods Mol Biol 132:365–386
36. Rudan I, Marušić A, Janković S, Rotim K, Boban M, Lauc G, Grković I, Đogaš Z, Zemunik T, Vatavuk Z, Benčić G, Rudan D, Mulić R, Krželj V, Terzić J, Stojanović D, Puntarić D, Bilić E, Ropac D, Vorko-Jović A, Znaor A, Stevanović R, Biloglav Z, Polašek O (2009) "10 001 Dalmatians:" Croatia launches its National Biobank. Croat Med J 50:4–6. doi:10.3325/cmj.2009.50.4
37. Schweigel-Röntgen M (2014) The families of zinc (SLC30 and SLC39) and copper (SLC31) transporters. In: Curr. Top. Membr. In: Bevens. Elsevier, Amsterdam, pp. 321–355
38. Simon DB, Lu Y, Choate KA, Velazquez H, Al-Sabban E, Praga M, Casari G, Bettinelli A, Colussi G, Rodriguez-Soriano J, McCredie D, Milford D, Sanjad S, Lifton RP (1999) Paracellin-1, a renal tight junction protein required for paracellular Mg2+ resorption. Science 285(5424):103–106
39. Takahashi N, Chernavvsky DR, Gomez RA, Igarashi P, Gitelman HJ, Smithies O (2000) Uncompensated polyuria in a mouse model of Bartter's syndrome. Proc Natl Acad Sci U S A 97:5434–5439. doi:10.1073/pnas.090091297
40. Thorleifsson G, Holm H, Edvardsson V, Walters GB, Styrkarsdottir U, Gudbjartsson DF, Sulem P, Halldorsson BV, de Vegt F, D'Ancona FCH, den Heijer M, Franzson L, Christiansen C, Alexandersen P, Rafnar T, Kristjansson K, Sigurdsson G, Kiemeney LA, Bodvarsson M, Indridason OS, Palsson R, Kong A, Thorsteinsdottir U, Stefansson K (2009) Sequence variants in the CLDN14 gene associate with kidney stones and bone mineral density. Nat Genet 41:926–930. doi:10.1038/ng.404
41. Toka HR, Genovese G, Mount DB, Pollak MR, Curhan GC (2013) Frequency of rare allelic variation in candidate genes among individuals with low and high urinary calcium excretion. PLoS One. doi:10.1371/journal.pone.0071885
42. Traglia M, Sala C, Masciullo C, Cverhova V, Lori F, Pistis G, Bione S, Gasparini P, Ulivi S, Ciullo M, Nutile T, Bosi E, Sirtori M, Mignogna G, Rubinacci A, Buetti I, Camaschella C, Petretto E, Toniolo D (2009) Heritability and demographic analyses in the large isolated population of val borbera suggest advantages in mapping complex traits genes. PLoS One 4:1–10. doi:10.1371/journal.pone.0007554
43. Tuschl K, Clayton PT, Gospe SM, Mills PB (2012) Dystonia/parkinsonism, hypermanganesemia, polycythemia, and chronic liver disease. In: Pragon RA et al. (ed) GeneReviews [Internet] Seattle (WA): University of Washington, Seattle; 1993–2016
44. Van Angelen AA, San-Cristobal P, Pulskens WP, Hoenderop JG, Bindels RJ (2013) The impact of dietary magnesium restriction on magnesiotropic and calciotropic genes. Nephrol Dial Transplant 28: 2983–2993. doi:10.1093/ndt/gft358
45. Vitart V, Rudan I, Hayward C, Gray NK, Floyd J, Palmer CNA, Knott SA, Kolcic I, Polasek O, Graessler J, Wilson JF, Marinaki A, Riches PL, Shu X, Janicijevic B, Smolej-Narancic N, Gorgoni B, Morgan J, Campbell S, Biloglav Z, Barac-Lauc L, Pericic M, Klaric IM, Zgaga L, Skaric-Juric T, Wild SH, Richardson WA, Hohenstein P, Kimber CH, Tenesa A, Donnelly LA, Fairbanks LD, Aringer M, McKeigue PM, Ralston SH, Morris AD, Rudan P, Hastie ND, Campbell H, Wright AF (2008) SLC2A9 is a newly identified urate transporter influencing serum urate concentration, urate excretion and gout. Nat Genet 40:437–442. doi:10.1038/ng.106
46. Wilcox ER, Burton QL, Naz S, Riazuddin S, Smith TN, Ploplis B, Belyantseva I, Ben-Yosef T, Liburd NA, Morell RJ, Kachar B, Wu DK, Griffith AJ, Riazuddin S, Friedman TB (2001) Mutations in the gene encoding tight junction claudin-14 cause autosomal recessive deafness DFNB29. Cell 104:165–172. doi:10.1016/S0092-8674(01)00200-8
47. Will C, Breiderhoff T, Thumfart J, Stuiver M, Kopplin K, Sommer K, Günzel D, Querfeld U, Meij IC, Shan Q, Bleich M, Willnow TE, Müller D, Günzel D, Querfeld U, Ic M, Shan Q, Bleich M (2010) Targeted deletion of murine Cldn16 identifies extra- and intrarenal compensatory mechanisms of Ca^{2+} and Mg^{2+} wasting. Am J Physiol Renal Physiol:1152–1161. doi:10.1152/ajprenal.00499.2009
48. Yu ASL (2015) Claudins and the kidney. J Am Soc Nephrol 26:11–19. doi:10.1681/ASN.2014030284